Letter | Editors' Suggestion

Corner universality in polygonal hydraulic jumps

S. I. Tamim [1,2] T. Nichols,[2] J. Lundbek Hansen [3] T. Bohr,[4] and J. B. Bostwick [2,*]

[1]*Department of Mathematics, University of North Carolina at Chapel Hill, Chapel Hill, North Carolina 27599, USA*

[2]*Department of Mechanical Engineering, Clemson University, Clemson, South Carolina 29634, USA*

[3]*SuperAI, Risk Analytics, Danske Bank, Laksegade 8, Copenhagen 1063, Denmark*

[4]*Department of Physics, Technical University of Denmark, DK-2800 Kongens Lyngby, Denmark*

(Received 18 August 2022; accepted 3 February 2023; published 7 March 2023)

Steady polygonal hydraulic jumps have a complex flow structure and are formed when a circular jump loses stability through an increase in the downstream liquid height beyond a critical value. We report the experimental observation of a universal corner shape in polygonal hydraulic jumps over a wide range of experimental conditions that include the flow rate, weir geometry, and flow history, as defined by the tip radius of curvature and the corner angle. The tip radius of curvature is nearly constant over all experimental conditions, whereas the corner angle weakly depends on gravitational effects. Knowledge of the corner angle allows one to determine the global jump shape, as defined by a dimensionless geometry number related to the isoperimetric inequality, thus giving a complete description of the jump shape.

DOI: 10.1103/PhysRevFluids.8.L032001

Hydraulic jumps are well-known phenomena in classical fluid mechanics, occurring whenever a flowing liquid layer undergoes an abrupt change in its vertical height, and can be observed over a large range of length scales, from the microfluidic flows used to sort red and white blood cells [1] to large-scale turbulent tidal bores [2,3]. Sustained scientific interest in hydraulic jumps can perhaps be linked to the fact that they are readily observed in everyday life as a "kitchen sink flow" [4–7]. Of particular note is the observation by Ellegaard *et al.* [8,9] of beautiful, steady polygonal hydraulic jumps with associated flow structure including a toroidal roller vortex located along the circumference of the jump that deforms and eventually breaks as the corner of the polygon is approached, resulting in a local vortex dipole there. Here the physics of pattern formation is complex, yet occurs over a small parameter range, and is often hysteretic [10]. Despite these complexities, we show in this Letter that the corner shape in polygonal hydraulic jumps is universal, as defined by the nearly constant tip radius of curvature and the corner angle that depends weakly upon gravitational effects.

The structure of a polygonal hydraulic jump is inherently multiphysics and involves the competition of surface tension, gravitational, inertial, and viscous forces. The connection with the well-known Plateau-Rayleigh instability of the circular jump base-state has been made by Bush *et al.* [11], thus highlighting the role of capillarity. However, the presence of the roller vortex in the downstream region makes this analogy complicated and few models have been proposed to analyze its role [12–14]. To further complicate matters is the fact that multiple polygons can be observed for the same experimental conditions, with this hysteresis highlighting the inherent nonlinearity in the problem [9,10,15]. Corners are formed where the roller vortex breaks up, giving rise to our

*jbostwi@clemson.edu

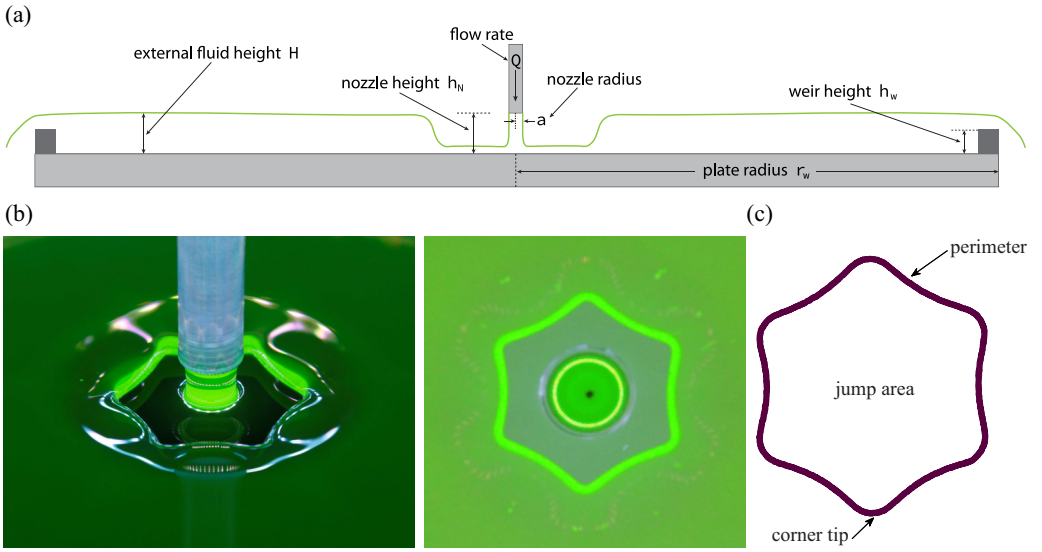

FIG. 1. (a) Schematic of the experimental setup used by Nichols and Bostwick [10] to generate (b) polygonal hydraulic jumps, shown here with $n = 6$ sides in perspective and bottom views. (c) The outline of the jump shape is determined through image processing and is defined by both the microscopic (corner tip) and macroscopic geometry (perimeter and area).

observation of a universal tip shape that is independent of flow rate, flow history, and weir geometry, thus suggesting a simpler description of the physics there.

Deformed interfaces often exhibit a local universal structure that is independent of the global physics governing the entire system that often result from a singularity in the governing equations and exhibit some degree of self-similarity [16,17]. Universality is defined by a local shape that remains invariant over large changes in the macroscopic system properties. Examples include the pinch off of liquid jets [18,19] and the formation of a sharp corner at a viscous fluid interface when fluid is drained from a bath [20,21], where the corner shape is regularized by a micron-sized tip curvature determined by a balance between surface tension and viscous forces only [22,23]. Universality can similarly be found in soft polymeric materials, such as the triangular-shaped "wetting ridge" which forms at the contact line of a partially-wetting drop/substrate system and remains invariant for static drops [24], as well as moving droplets [25].

In the case of polygonal hydraulic jumps, the local corner shape is universal but the global jump shape is not, i.e., the area A, the perimeter P, and the number of corners n change with experimental parameters. Nevertheless, we find that normalized global geometry, as defined by the geometry number $G \equiv P/\sqrt{A}$, has a universal feature that can be understood through an analogy with the shape of two-dimensional bubbles in dry foams. The shape of a bubble in a two-dimensional (2D) foam is determined by free energy minimization (isoperimetric problem) with boundary conditions enforced from Plateau's laws of foams that dictates the angle between adjoining interfaces should be 120°, with Graner *et al.* [26] having computed G against n for this case showing that $G \to 3.73$ as $n \to \infty$. For polygonal hydraulic jumps, our normalized experimental data are strikingly close to those of 2D bubbles in dry foams with the difference being explained by the observation that our corner angle deviates slightly from 120°. This further highlights the role of surface tension in determining the jump shape and suggests that the entire polygonal jump shape (local and global geometry) can be determined from the tip geometry through patching.

Experiment. Polygonal hydraulic jumps are made using the experimental setup shown in Fig. 1(a). Fluid flows through a nozzle of radius $a = 0.45$ cm at a flow rate of $Q = 30$–110 mL/s and vertically impinges upon a circular glass plate of radius $r_w = 12.7$, 15.24, and 17.78 cm, which

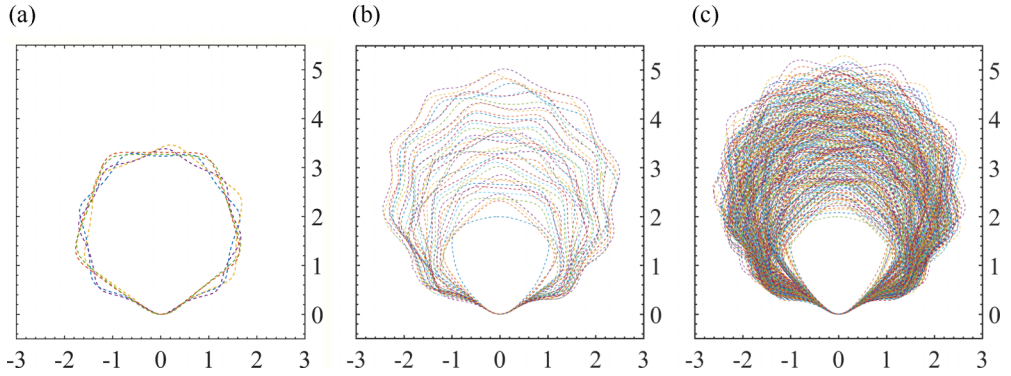

FIG. 2. Overlaid hydraulic jump shapes exhibit a hierarchy of corner universality, as illustrated for (a) fixed flow rate $Q = 55.5$ mL/s and weir geometry $r_w = 12.7$ cm and $h_w = 2.84$ mm ($n = 5$–8); (b) fixed weir geometry $r_w = 15.2$ cm and $h_w = 2.84$ mm, and varying flow rate Q ($n = 3$–10); and (c) varying both flow rate and weir geometry ($n = 3$–10). The units on the axes are centimeters with corner tips located at the origin (0,0).

has a weir of height $h_w = 2.67$, 2.84, and 3.12 mm affixed to the outer edge so as to increase the external fluid height [H in Fig. 1(a)] and create the "free-fall effect." The fluid spreads radially outward from the central jet in a rapid, shallow ("supercritical") layer until it reaches the jump region, where the fluid height abruptly increases resulting in a hydraulic jump like that shown in Fig. 1(b). Ethylene glycol was the working fluid with the following material properties: viscosity $\nu = 13.7$ mm^2/s, density $\rho = 1.12$ g/cm^3, and surface tension $\sigma = 44$ mN/m. Polygonal hydraulic jumps are characterized by the number of corners (equivalently, sides) n and the macroscopic geometry through the area A and the perimeter P [cf. Fig. 1(c)], which are computed using the image-processing techniques described in Nichols and Bostwick [10]. The jump shape is sensitive to both the material and experimental parameters, as well as the experimental protocol. We use two distinct protocols: (i) upscale-downscale and (ii) natural state. For fixed weir geometry h_w and r_w, the upscale-downscale protocol involved slowly increasing the flow rate Q in increments of 1 mL/s and observing the changes in polygonal shape from $n \to n + 1$ until the maximum flow rate was reached (upscale), after which Q was decreased in increments of 1 mL/s, resulting in $n \to n - 1$ transitions (downscale). This protocol exhibits hysteresis and it is possible to observe shapes with different n for the same flow rate. The natural state protocol is similar except the jump shape was destroyed at each flow rate increment and allowed to relax to its preferred state by eliminating the effect of flow history. More details on the experimental method can be found in Nichols and Bostwick [10].

Results. Polygonal jumps show a remarkable universality in the corner shape, which we illustrate in Fig. 2 by overlaying jump shapes and aligning them on a common corner. The choice of which corner to align was inconsequential due to the high degree of symmetry of each polygonal shape. We define the different universality classes. Figure 2(a) exhibits the strongest universality obtained for a fixed flow rate Q and the weir geometry h_w and r_w showing polygonal jumps with $n = 5$–8 have the same corner geometry in a region that spans a width of approximately 0.6 cm from the tip of the corner. Note that these shapes were data mined from both upscale-downscale protocols and natural state protocols. Figure 2(b) shows the corner universality for fixed weir geometry with the natural state protocol, over a range of flow rates for 41 different polygons with $n = 3$–10 sides. In this case, the similarity tends to persist for up to a width of 0.4 cm from the tip of the corner. Here, the higher-order polygons, i.e., those with $n \geqslant 6$, show much stronger universality compared to lower-order polygons. Finally, Fig. 2(c) plots all of our data from the natural state protocol with variations in both the flow rate and the weir geometry, for a total of 335 jump shapes with $n = 3$–10 sides. For this large data set, the corner universality is slightly reduced from the previous cases, as

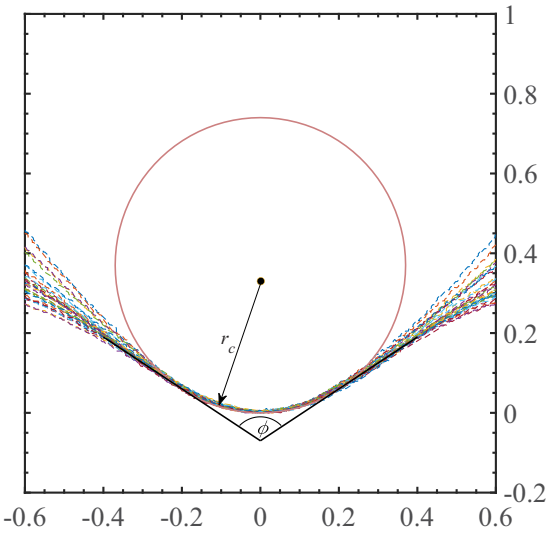

FIG. 3. Universal corner shape is defined by the radius of curvature r_c and the corner angle ϕ, as defined by the intersection of the tangent lines along the straight edges of the corner, as shown here for the weir geometry $r_w = 12.7$ cm and $h_w = 2.84$ mm with best fits $r_c = 3.7$ mm and $\phi = 114^\circ$.

might be expected given the larger range of experimental parameters, but is still clearly apparent. We quantify this corner universality through the tip radius of curvature r_c and the corner angle ϕ, as shown in Fig. 3. Here r_c essentially defines the local corner geometry and ϕ the global geometry of the polygonal jump; the connection between them we discuss later. Figure 3 shows a case of fixed weir geometry and varying flow rate for 29 shapes with $n = 3$–10, where r_c is nearly constant with a best fit of $r_c = 3.7$ mm and the corner angle is $\phi = 114 \pm 2^\circ$. We find that $r_c = 3.5 \pm 0.2$ mm over our entire data set. Hysteresis has some effect on r_c for lower-order polygons $n \leqslant 4$ which can become strongly curved and deviate from this universal value. In contrast to the tip radius of curvature, the corner angle ϕ defines the intermediate (or matching) region between the tip and the global jump shape, and we might expect it to depend weakly on the experimental parameters. This is summarized in Table I. For fixed weir geometry and variation in flow rate, ϕ remains nearly constant with a deviation of 4° between protocols at worst and indistinguishable at best. For a fixed weir radius r_w, increasing the weir height h_w tends to decrease the corner angle ϕ. As increases in the

TABLE I. Corner angle $\phi[^\circ]$, as it depends upon experimental parameters r_w and h_w and the protocol (natural, upscale, and downscale), shown as an average value with a maximum deviation of $\pm 3^\circ$ over each respective data set.

r_w (cm)	h_w (cm)	Natural	Upscale	Downscale
12.7	2.67	114	114	114
12.7	2.84	114	114	114
12.7	3.17	110	114	113
15.24	2.67	118	118	118
15.24	2.84	118	118	118
15.24	3.17	110	111	111
17.78	2.67	118	120	119
17.78	2.84	118	119	118
17.78	3.17	110	113	110

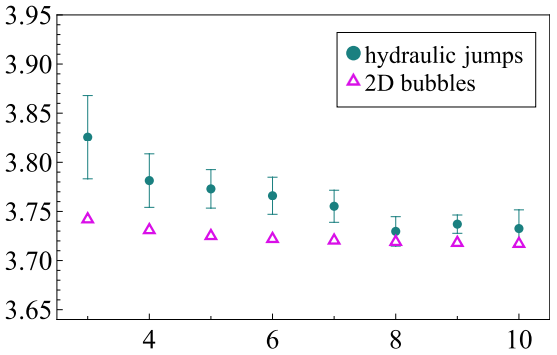

FIG. 4. Analogy between macroscopic geometry of polygonal jumps and bubbles in 2D foams by plotting the geometry number $G = P/\sqrt{A}$ against the side number n for polygonal jumps (circles, all data) and 2D bubbles (triangles) [26]. Error bars represent the 95% confidence interval for average over all different data sets.

weir height lead to increases in the downstream jump height, this indicates that gravitational effects may play a role in selection of the corner angle. Given the universality of the corner shape defined by r_c and ϕ, one can further speculate that the global jump geometry, as defined by the area A and the perimeter P, also exhibits some universality. The global shape geometry can be normalized into a dimensionless geometry number $G \equiv P/\sqrt{A}$ related to the isoperimetric inequality. Figure 4 plots the geometry number G against n for all of our data which exhibit a decreasing trend that plateaus to $G \approx 3.73$ for large n. The connection to the isoperimetric problem suggests an analogy between the polygonal hydraulic jump shapes and the theoretical shapes of two-dimensional bubbles in dry foams, where each bubble shares its corners with neighboring bubbles [27]. It is well-known from Plateau's law that the bubble edges of a dry foam meet at an angle of 120° [28] and that the interfaces are circular arcs. With these rules Graner *et al.* [26] computed the bubble shapes for the corner angle 120°, as it depends upon the number of corners n, and we compare the normalized geometry G with polygonal hydraulic jumps in Fig. 4. Here we note the qualitative trends are similar but the value of G for polygonal jumps is always larger than that for 2D bubbles, although they approach similar values for large n ($G \approx 3.73$ for foams). This difference is presumably due to the respective corner angle that is enforced. The corner angles ϕ for polygonal jumps are always lower than the Plateau angle $\phi = 120°$ and this difference can be as large as 10° (cf. Table I). It is, therefore, reasonable to expect some difference in the respective geometry numbers G, especially whenever the number of corners is small. For example, $G = 3.82$ for $n = 3$ polygons, whereas $G = 3.74$ for $n = 3$ bubbles. The similarity in G increases for higher-order polygons, e.g., $n \geqslant 8$, and we note this is also within the range of n which shows the strongest corner universality (cf. Fig. 2). This global feature also appears in mode number n selection by defining the instability wavelength $\lambda = P/nH$, which assumes a constant value at large n (cf. Nichols and Bostwick [10, Fig. 10]). This is similar to the Plateau-Rayleigh instability, suggesting the formation of polygonal jumps is a primarily capillary-driven instability, at least for cases with $n \geqslant 6$ where the sides are highly curved.

Discussion. In this work we have experimentally revealed a universality in the corner shape of polygonal hydraulic jumps over a large range of parameters, as defined by the radius of curvature $r_c = 3.5 \pm 0.2$ mm and the corner angle $\phi = 115 \pm 5°$. There is a matching region that connects the local corner geometry (inner region) to the global polygonal geometry (outer region), which is largely determined by the geometry number G related to the isoperimetric inequality that enables us to reconstruct the entire polygonal jump shape.

Polygonal jumps are formed when the downstream toroidal roller vortex undergoes a varicose instability that is too large to sustain a uniform toroidal shape and destabilizes with corners appearing in the region where vortex breakup occurs [12,29]. We find that variation in the upstream flow velocity does not affect the corner geometry, even though it has a significant effect on the

geometry of circular hydraulic jumps [6]. The process is qualitatively similar to Plateau-Rayleigh breakup of liquid toroids which is known to give rise to a self-similar shape near the pinchoff region [30–33]. Our observations also show a self-similar corner region, although without collapse as with a fluid torus or vortex ring [34]. In a somewhat related study, universality has been observed in the corner shape of solitonlike waves on the surface of a Leidenfrost-levitated toroid with the curvature depending upon the mode number n (Perrard *et al.* [35, Fig. 4c]), which is markedly different from our observations where the curvature is independent of n. Free surface cusp singularities have been observed in low Reynolds number flows and are dominated by a balance between surface tension and viscous forces [22,23,36]. The presence of a vortex dipole is often associated with such flows where the convergence of two vortices corotating at a sufficiently high speed generates the cusp and the same is true for polygonal hydraulic jumps, as clearly shown in Bush *et al.* [11, Fig. 5]. Jeong and Moffatt [22] have used a theoretical analysis to show that the tip curvature on a free surface cusp scales logarithmically with the capillary number due to the vortices. Similarly, in polygonal hydraulic jumps, vortex dipoles appear spontaneously near the corners where the toroidal roller breaks. The hydraulic jumps we report here are distinguished by a large Reynolds number $\mathrm{Re} \equiv Q/\nu a = 450$–$1350$ and a small Ohnesorge number $\mathrm{Oh} \equiv \nu/\sqrt{\sigma h/\rho} = 0.028$–$0.031$, indicating small viscous effects and nontrivial inertial effects from this vastly different flow regime [37]. We note Bush *et al.* [11, Fig. 6] were able to suppress the corner shape through the addition of surfactant into the flow, further highlighting the prominent role of surface tension in determining the corner shape. The Bond number for our system $\mathrm{Bo} \equiv \rho g(\Delta h)^2/\sigma = 7.5$–$10.5$ is order one such that the surface tension and gravitational forces are of similar magnitude and this balance defines the capillary length $\ell_c = \sqrt{\sigma/\rho g} = 2$ mm, which is of similar size to r_c.

We can give a very rough estimate of the size of r_c by considering an extension of the Rayleigh-Bélanger jump condition treating the jump as a stationary shock and equating flux and momentum flux across the shock. The momentum flux density is $\int_0^h [p(r,z) + \rho u^2(r,z)]\,dz$, with the pressure $p(r,z)$ and the flow velocity $u(r,z)$, and the extended Rayleigh-Bélanger condition is obtained by assuming the pressure is the sum of the hydrostatic pressure $p_g = \rho g[h(r) - z]$ and the capillary pressure from the curved outer surface $p_\sigma \approx -\sigma/r_c$, such that $p(r,z) = p_g + p_\sigma$. If we replace the velocity $u(r,z)$ by its mean value $v(r) = \frac{1}{h(r)} \int_0^{h(r)} u(r,z)dz$, we get

$$\frac{1}{2}\rho g h_1^2 + \rho h_1 v_1^2 = \frac{1}{2}\rho g h_2^2 + \rho h_2 v_2^2 - \frac{\sigma h_2}{r_c}, \tag{1}$$

which is the standard Rayleigh-Bélanger condition when $\sigma = 0$, with h_1 being the upstream height, h_2 the downstream height, v_1 the upstream mean velocity, and v_2 the downstream mean velocity, respectively. The change in the fluid height can be defined as $\Delta h \equiv h_2 - h_1$. Note this is different from the jump condition with surface tension for a circular hydraulic jump derived by Bush and Aristoff [38]. Since $h_1 \ll h_2 \approx \Delta h$ we can approximate Eq. (1) as

$$\frac{\Delta h}{r_c} = \frac{1}{2}\left(\frac{\Delta h}{l_c}\right)^2 - \frac{\rho}{\sigma}\left(h_1 v_1^2 - h_2 v_2^2\right) = \frac{1}{2}\mathrm{Bo} - (\mathrm{We}_1 - \mathrm{We}_2) \tag{2}$$

where $\mathrm{We} = \frac{\rho h v^2}{\sigma}$ is the local Weber number. The inner flow is axially symmetric such that

$$\mathrm{We}_1 = \frac{\rho}{\sigma}\frac{h_1 Q^2}{(2\pi r_J h_1)^2} = \frac{\rho Q^2}{(2\pi r_J)^2 \sigma h_1}, \tag{3}$$

where r_j is the radius of the jump in the corner. For example, when $Q \approx 50$ mL/s, $h_1 \approx 0.5$ mm, and $r_j \approx 2$ cm, then $\mathrm{We}_1 \approx 8$. If the outer flow retained the axial symmetry, we would have a similar expression for We_2; however, the flow on the outer side is far from axially symmetric and is strongly concentrated near the corners in "jets" as clearly shown in Fig. 5, reproduced from Ref. [12]. Accordingly, we do not know how to give an accurate value of r_c from Eq. (2), but we

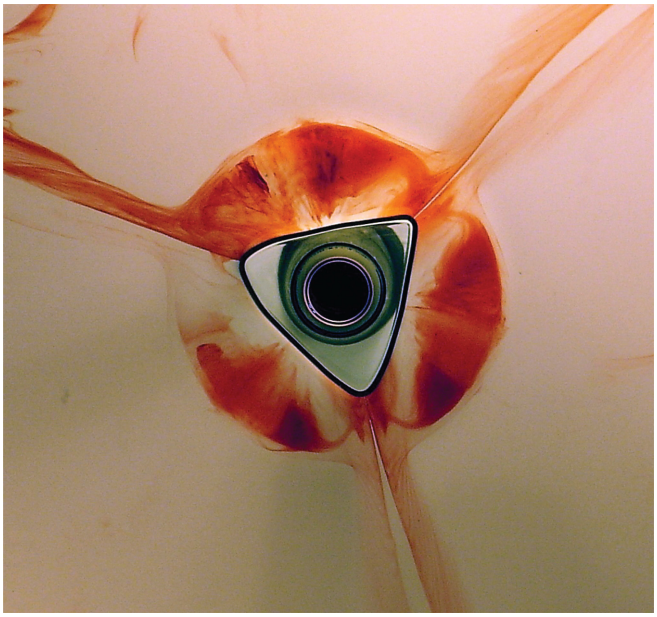

FIG. 5. Hydraulic triangle $n = 3$ on a glass plate seen from below, reproduced with permission from Ref. [12], with the outgoing jets at the corners clearly shown.

can provide a lower bound on r_c (since $\mathrm{We}_2 < \mathrm{We}_1$) by neglecting the kinetic terms:

$$r_c > \frac{2\Delta h}{\mathrm{Bo}} = \frac{2l_c^2}{\Delta h} \approx 0.58 l_c - 0.74 l_c. \tag{4}$$

Including the kinetic terms could substantially increase this estimate, but why r_c determined in this way would be independent of flow rate remains a mystery. Here, presumably, the viscosity plays a large role in determining the structure of the vortices meeting at the corner, and thereby the strength of the jets. In fact, the Reynolds number in the jump region $\mathrm{Re}_J \approx v_2 \Delta h/\nu \approx Q/(2\pi r_J \nu)$ is around 50, suggesting we have a complex flow between the solid substrate and strongly deformed surface, where gravity, inertia, viscosity, and surface tension are all important.

Lastly, we note the strong analogy made between the theory of 2D bubble shapes in foams and the global geometry of polygonal jumps and how this is intimately related to knowledge of the corner shape. This is important because whenever the corner shape is fixed, the rest of the jump structure is determined through simple geometry. Therefore, understanding of the physical mechanism underlying the corner shape should provide key insights about the complex physics of polygonal hydraulic jump formation. Our experiments can be viewed as simple kitchen sink flows, yet these hydraulic jumps could potentially be used as a test bed for analyzing similar large-scale systems, i.e., gas dynamic shock waves [39] and open channel flows [40], or can simply be used as an educational tool to introduce and describe universality and singularities in a macroscopic system.

Acknowledgments. The idea of the corner universality and the use of the Geometry number G originated many years ago, in the Ph.D. thesis [41] by one of us (J.L.H.).

[1] H. Shirinkami, G. Wang, J. Park, J. Ahn, Y. Choi, and H. Chun, Red blood cell and white blood cell separation using a lateral-dimension scalable microchip based on hydraulic jump and sedimentation, Sens. Actuators, B **307**, 127412 (2020).

[2] X. Leng and H. Chanson, Breaking bore: Physical observations of roller characteristics, Mech. Res. Commun. **65**, 24 (2015).
[3] C. Gualtieri and H. Chanson, Experimental analysis of Froude number effect on air entrainment in the hydraulic jump, Environ. Fluid Mech. **7**, 217 (2007).
[4] L. Rayleigh, On the theory of long waves and bores, Proc. R. Soc. London A **90**, 324 (1914).
[5] E. J. Watson, The radial spread of a liquid jet over a horizontal plane, J. Fluid Mech. **20**, 481 (1964).
[6] T. Bohr, P. Dimon, and V. Putkaradze, Shallow-water approach to the circular hydraulic jump, J. Fluid Mech. **254**, 635 (1993).
[7] A. Duchesne, A. Andersen, and T. Bohr, Surface tension and the origin of the circular hydraulic jump in a thin liquid film, Phys. Rev. Fluids **4**, 084001 (2019).
[8] C. Ellegaard, A. E. Hansen, A. Haaning, K. Hansen, A. Marcussen, T. Bohr, J. L. Hansen, and S. Watanabe, Creating corners in kitchen sinks, Nature (London) **392**, 767 (1998).
[9] C. Ellegaard, A. E. Hansen, A. Haaning, K. Hansen, A. Marcussen, T. Bohr, J. L. Hansen, and S. Watanabe, Cover illustration: Polygonal hydraulic jumps, Nonlinearity **12**, 1 (1999).
[10] T. E. Nichols and J. B. Bostwick, Geometry of polygonal hydraulic jumps and the role of hysteresis, Phys. Rev. Fluids **5**, 044005 (2020).
[11] J. W. M. Bush, J. M. Aristoff, and A. E. Hosoi, An experimental investigation of the stability of the circular hydraulic jump, J. Fluid Mech. **558**, 33 (2006).
[12] E. A. Martens, S. Watanabe, and T. Bohr, Model for polygonal hydraulic jumps, Phys. Rev. E **85**, 036316 (2012).
[13] M. Labousse and J. W. M. Bush, The hydraulic bump: The surface signature of a plunging jet, Phys. Fluids **25**, 094104 (2013).
[14] N. Rojas and E. Tirapegui, Harmonic solutions for polygonal hydraulic jumps in thin fluid films, J. Fluid Mech. **780**, 99 (2015).
[15] A. R. Teymourtash and M. Mokhlesi, Experimental investigation of stationary and rotational structures in non-circular hydraulic jumps, J. Fluid Mech. **762**, 344 (2015).
[16] J. Eggers and M. A. Fontelos, *Singularities: Formation, Structure, and Propagation*, Cambridge Texts in Applied Mathematics Vol. 53 (Cambridge University, Cambridge, England, 2015).
[17] G. I. Barenblatt, *Scaling, Self-Similarity, and Intermediate Asymptotics: Dimensional Analysis and Intermediate Asymptotics*, Cambridge Texts in Applied Mathematics Vol. 14 (Cambridge University, Cambridge, England, 1996).
[18] J. Eggers, Universal Pinching of 3D Axisymmetric Free-Surface Flow, Phys. Rev. Lett. **71**, 3458 (1993).
[19] D. T. Papageorgiou, On the breakup of viscous liquid threads, Phys. Fluids **7**, 1529 (1995).
[20] S. Courrech du Pont and J. Eggers, Sink Flow Deforms the Interface Between a Viscous Liquid and Air into a Tip Singularity, Phys. Rev. Lett. **96**, 034501 (2006).
[21] E. Lorenceau, F. Restagno, and D. Quéré, Fracture of a Viscous Liquid, Phys. Rev. Lett. **90**, 184501 (2003).
[22] J.-T. Jeong and H. K. Moffatt, Free-surface cusps associated with flow at low Reynolds number, J. Fluid Mech. **241**, 1 (1992).
[23] S. C. du Pont and J. Eggers, Fluid interfaces with very sharp tips in viscous flow, Proc. Natl. Acad. Sci. USA **117**, 32238 (2020).
[24] R. W. Style, R. Boltyanskiy, Y. Che, J. S. Wettlaufer, L. A. Wilen, and E. R. Dufresne, Universal Deformation of Soft Substrates Near a Contact Line and the Direct Measurement of Solid Surface Stresses, Phys. Rev. Lett. **110**, 066103 (2013).
[25] S. J. Park, J. B. Bostwick, V. De Andrade, and J. H. Je, Self-spreading of the wetting ridge during stick-slip on a viscoelastic surface, Soft Matter **13**, 8331 (2017).
[26] F. Graner, Y. Jiang, E. Janiaud, and C. Flament, Equilibrium states and ground state of two-dimensional fluid foams, Phys. Rev. E **63**, 011402 (2000).
[27] I. Cantat, S. Cohen-Addad, F. Elias, F. Graner, R. Höhler, O. Pitois, F. Rouyer, and A. Saint-Jalmes, *Foams: Structure and Dynamics* (Oxford University, Oxford, 2013).
[28] J. Plateau, *Statique Expérimentale et Théorique des Liquides Soumis aux Seules Forces Moléculaires*, Vol. 2 (Gauthier-Villars, Paris, 1873).

[29] M. Labousse and J. W. M. Bush, Polygonal instabilities on interfacial vorticities, Eur. Phys. J. E **38**, 113 (2015).
[30] J. Eggers and T. F. Dupont, Drop formation in a one-dimensional approximation of the Navier–Stokes equation, J. Fluid Mech. **262**, 205 (1994).
[31] E. Pairam and A. Fernández-Nieves, Generation and Stability of Toroidal Droplets in a Viscous Liquid, Phys. Rev. Lett. **102**, 234501 (2009).
[32] J. D. McGraw, J. Li, D. L. Tran, A.-C. Shi, and K. Dalnoki-Veress, Plateau-Rayleigh instability in a torus: Formation and breakup of a polymer ring, Soft Matter **6**, 1258 (2010).
[33] J. B. Bostwick and P. H. Steen, Stability of constrained cylindrical interfaces and the torus lift of Plateau–Rayleigh, J. Fluid Mech. **647**, 201 (2010).
[34] S. E. Widnall and J. P. Sullivan, On the stability of vortex rings, Proc. R. Soc. London A **332**, 335 (1973).
[35] S. Perrard, Y. Couder, E. Fort, and L. Limat, Leidenfrost levitated liquid tori, Europhys. Lett. **100**, 54006 (2012).
[36] D. D. Joseph, J. Nelson, M. Renardy, and Y. Renardy, Two-dimensional cusped interfaces, J. Fluid Mech. **223**, 383 (1991).
[37] A. Duchesne, L. Lebon, and L. Limat, Constant Froude number in a circular hydraulic jump and its implication on the jump radius selection, Europhys. Lett. **107**, 54002 (2014).
[38] J. W. M. Bush and J. M. Aristoff, The influence of surface tension on the circular hydraulic jump, J. Fluid Mech. **489**, 229 (2003).
[39] A. R. Kasimov, A stationary circular hydraulic jump, the limits of its existence and its gasdynamic analogue, J. Fluid Mech. **601**, 189 (2008).
[40] H. Chanson, Current knowledge in hydraulic jumps and related phenomena: A survey of experimental results, Eur. J. Mech.-B/Fluids **28**, 191 (2009).
[41] J. L. Hansen, Pattern formation of sand ripples and polygons in the hydraulic jump, Ph.D. thesis, Copenhagen, Denmark, 2001.